British Journal of Environmental Sciences
Vol.2, No.4, pp.29-40, December 2014
Published by European Centre for Research Training and Development UK (www.eajournals.org)

IMPROVEMENT OF TITANIUM DIOXIDE NANOTUBES THROUGH STUDY WASHING EFFECT ON HYDROTHERMAL

Amr Nada (Corresponding author)
Egyptian Petroleum Research Institute, EPRI, Cairo, Egypt.

Yasser Moustafa and Amal Hamdy
Egyptian Petroleum Research Institute, EPRI, Cairo, Egypt.
Saad Abd El-Wahab and Dena Yahea
Ain shams Univeristy Cairo, Egypt.

ABSTRACT: *Titanate nanotubes (TNT) were prepared via a hydrothermal treatment of synthesized* TiO_2 *powders in a 10 M NaOH solution at 130 ◦C for 24 h and subsequently washed with HCl aqueous solution of different concentrations (with water only, 0.01, 0.1 and 1 M). Samples with different contents of remnant sodium in nanotubes after heat-treatment were characterized, by high resolution transmission electron microscopy, X-ray diffraction, fourier transform infrared spectroscopy and Raman spectroscopy. The photocatalytic activity of TNT was evaluated by photocatalytic oxidation of phenol in water solution. Highly remnant sodium in nanotubes has a detrimental effect on the photocatalytic activity of titanate. This is attributed to the high concentration sodium preventing formation of the photoactive anatase phase and low concentration sodium producing surface and bulk recombination centers of photogenerated electron-hole pairs.*

KEYWORDS: Titanium Dioxide Nanotubes. Washing, Hydrothermal

INTRODUCTION

In recent years, semiconductor photocatalytic process has shown a great potential as a low-cost, environmental friendly and sustainable treatment technology, especially titanium dioxide semiconductor. The selection of titania is due to its strong oxidizing power, nontoxicity, biological and chemical inertness, and long-term stability against photo and chemical corrosion (Fox and Dulay, 1993). However, one main obstacle for the widespread commercial application of photocatalytic oxidation technology is the low photocatalytic efficiency of TiO_2 (Lin and Yu, 1998). Therefore, it is an important and interesting task to improve the photocatalytic activity of TiO_2 by different chemical and physical methods (Sun et al., 2002; Tseng et al., 2002; Yamashita et al., 2002). Kasuga et al. (1998, 1999) reported the preparation of titanate by a simple hydrothermal treatment. However, it was found that the titanate were easily affected by the preparation conditions, including such variables as reaction time, synthesis temperature, acid washing concentration and calcination temperature (Kasuga, 2006; Lee et al., 2007b; L. Q. Weng et al., 2006; Yoshida et al., 2005; Yu et al., 2006a,b,c), which in turn may have significant effects on the photocatalytic activity of TNT. For instance, several groups have reported that the TiO_2

nanotubes may possess better (Yu et al., 2006a,b) or worse (Zhang et al., 2004) photocatalytic activity with the comparison to colloidal or other forms of titanate.
The inconsistency in the conclusions for the photocatalytic activity of TNT may be due to the difference in the synthetic conditions for the preparation of TNT samples. Therefore, to clearly clarify the synthetic conditions for the preparation of TNT samples with highly photocatalytic activity should be important from the point of view of practical use. In this study, effect of washing parameters, on the photocatalytic degradation of phenol performance of TNT, prepared by the hydrothermal method, are examined. The synthetic parameters for the preparation of TNT samples with highly photocatalytic activity are then determined.

EXPERIMENTAL

Preparation of TiO_2 nanoparticles

All chemicals were of analytical grade and used without further purification.TiO_2 nanoparticles were prepared by the method of hydrolysis as reported by (S.S. Kanmani and K. Ramachandran, 2012) with little modification. Titanium (IV) isopropoxide (Ti [OCH (CH3)$_2$]$_4$) was used as a starting precursor. Typically, 7 ml of Ti $[OCH(CH_3)_2]_4$ was dissolved in 100 ml of isopropyl alcohol $[(CH_3)_2CHOH]$ and the solution was stirred continuously for 1 hour at room temperature. After stirring, 400 ml of deionized water was added suddenly to the above prepared mixture. The resultant solution was aged for 3 hours, then centrifuged, washed several times with deionized water and ethanol and dried at 80 ^oC over night. The preparation of the TiO_2 nanoparticles was then completed by calcinating the precipitated particles at 450 ^oC for 2 hours in air.

Preparation of TiO_2 nanotubes (TNTs)

TNTs were prepared by the modified hydrothermal method (Li 2009). In a typical run, 2 g TiO_2 powder was added into 50 mL of 10 mol/L NaOH aqueous solution and the suspension system was stirred for 1 h at room temperature to form a suspension. Then, the mixture was transferred to a Teflon-lined stainless steel autoclave at 130 ^oC for 24 hour. After cooled naturally in air, the mixture was centrifuged at a speed of 4000 rpm and the precipitates were collected. The white powder was thoroughly washed with HCl aqueous solution of different concentrations (with water only, 0.01, 0.1 and 1 M) are labeled as TN-W, TN-0.01MC, TN-0.1MC and TN-1MC respectively, followed by drying at 80 ^oC. All samples were prepared will under calcination for 4 hour at 450 ^oC.

Characterization of TiO_2 nanotube

The morphology of samples was investigated by High Resolution Transmission Electron Microscope (HRTEM). Model JEM-2100, JEOL, Japan. A small quantity of used catalysts were dispersed in 10 ml ethanol then sonicated for 30 min. Few drops of the resulting suspension were placed on a covered copper grid and photographed at acceleration rate of 200 KV.Energy dispersive x-ray analysis (EDX), was carried out by TEM-EDX (model JEM-2100, JEOL, Japan). The results of the elemental analyses of titanate are useful in giving a hint of relative proportions of the different components

Selected area electron diffraction (SAED), Diffraction patterns analysis is an excellent complement to x-ray diffraction data by HRTEM (model JEM-2100, JEOL, Japan). Diffraction patterns provide structural details related to the specimen's orientation, polytype, phase, and defect morphology.The studied samples were examined using X-ray powder diffractometer, Panalytical XPERT PRO MPD. Cu Kα radiation (λ= 1.5418 A°) was used at a rating of 40 kV, 40 mA. The diffraction patterns were recorded at room temperature in the angular range of 4°-80° (2θ) with step size 0.02° (2θ) and scan step time 0.4 (s). The crystalline phases, in both cases, were identified using the ICDD-PDF database.

Fourier transform infrared spectroscopy (FTIR), The FTIR spectra in the 4000-400 cm^{-1} range were recorded for the prepared nanomaterials at room temperature by Perkin Elmer (model spectrum one FT-IR spectrometer, USA). Samples were prepared using the standard KBr pellets. Raman spectra of the samples were recorded on the dispersive Raman microscope (model Sentera, Bruker, Germany) instrument at laser wave length 532 nm [doubled Nd:YAG laser (neodymium-doped yttrium aluminum garnet)] and power 10 mW. A Perkin Elmer UV/vis Spectrophotometer (Model: Lambda 1050) was used for the measurement of absorbance over the wavelength range of 200 nm to 800 nm. Photoluminescence (PL) spectrum at room temperature was recorded using spectrofluorophotometer (RF-5301 PC, Japan, SHIMADZU, 400 W, 50/60 Hz).

Photocatalytic reactions

Photocatalytic reaction was conducted in a commercial photo-reactor equipped with a 500 ml cylindrical Pyrex vessel irradiated directly by an ultra violet lamp has wave length (365 nm). For photocatalytic phenol degradation, 0.2 g of the catalyst was mixed with 500 ml of 50mg/l phenol solution which was further stirred in the dark for 30 min to reach the adsorption equilibrium prior to the photocatalytic test. During the photocatalytic reaction, samples were collected at selected time intervals and the catalyst particles were removed by centrifugation. The residual phenol concentration was determined using HPLC (Agilent 1200, USA), equipped with an ultraviolet (UV) detector and a C18 reversed phase column (250mm×4.5mm, Agilent, USA) at 30 °C. The mobile phase consists of water and acetonitrile (40/60, v/v) with a flow rate of 1.0 ml min^{-1}.

RESULTS AND DUSCUSSION

Titanate was washed with different concentrations of HCl aqueous solution. TEM images of TN-W, TN-0.01MC, TN-0.1MC and TN-1MC samples are shown in Fig 1. According to HRTEM observations, the morphological characteristics of TN-0.01MC and TN-0.1MC show that both samples are rather similar nanotubes with a diameter of 7-10 nm and a length of 50-80 nm. For TN-1MC the nanotubular structure becomes diffused and the length of TNT becomes shorter however the sample without washing by HCl, TN-W, the nanotubular structure shows uncompleted formation. Selected area electron diffraction (SAED) in case of TN-0.1MC and TN-0.01MC appear as single crystal refers to best case of formation nanotubular structure but in case TN-w and TN-1MC less purity of single crystal was obtained due to uncompleted titanate structure.

Energy dispersive x-ray analysis (EDX) referred to the presence of sodium in titanate structure in a sequence as shown in Table 1. This measured by Quantitation method: Cliff Lorimer thin ratio section. It can be noticed that on increasing the HCl concentration the weight percent of sodium decreases. If we assume that there have two kinds of sodium ions in the TNT: (i) ions to form the crystal and (ii) free ions trapped in the pore structure this confirmed by XRD.

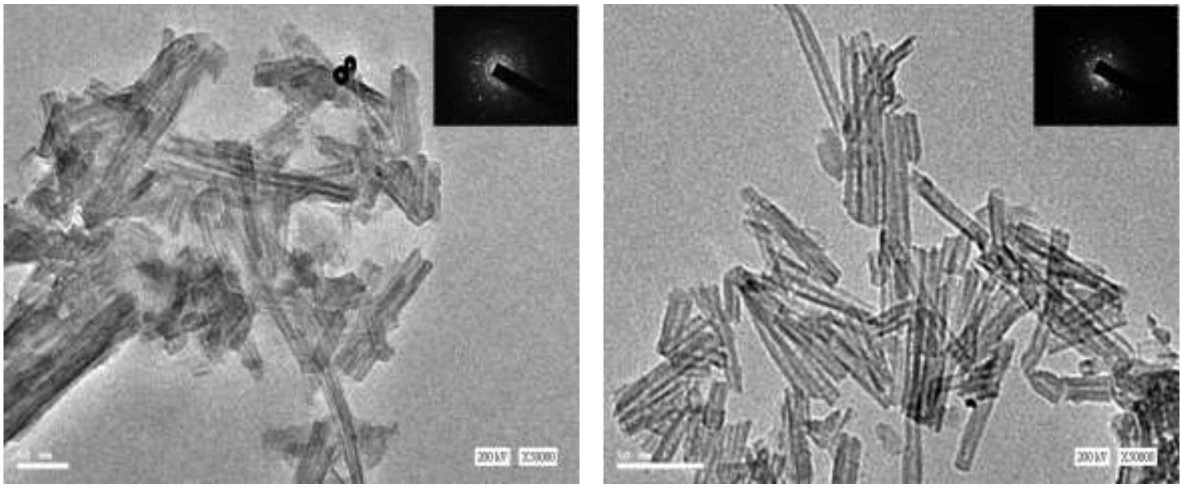

Fig 1.a. TN-W Fig 1.b. TN-0.01MC

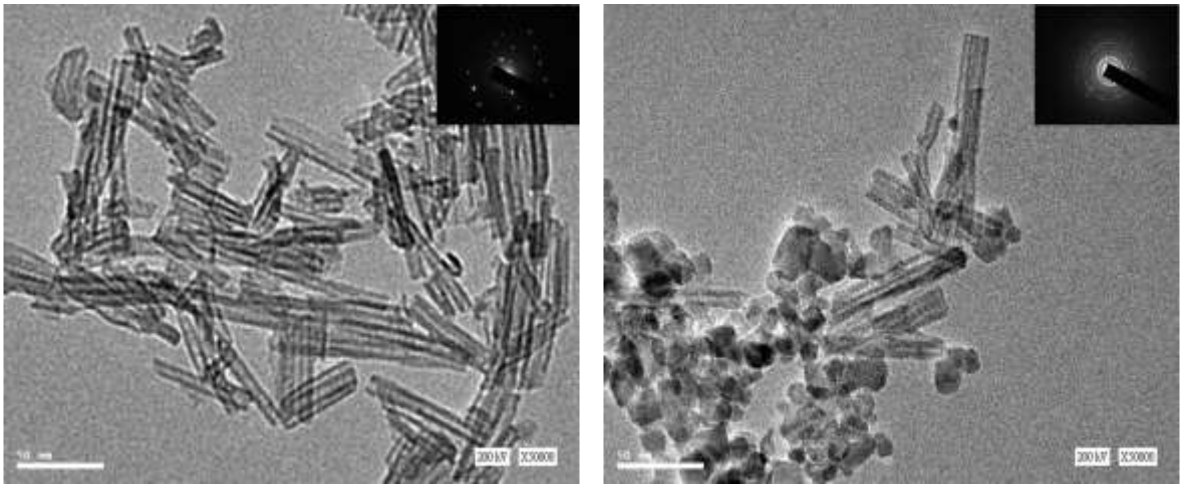

Fig 1.c. TN-0.1MC Fig 1.d. TN-1MC

Fig. 1: HRTEM images and electron diffraction patterns of prepared samples.

	TN-W	TN-0.01MC	TN-0.1MC	TN-1MC
Element	Weight %	Weight %	Weight %	Weight %
Na K	7.72	5.61	3.57	0.0
Ti K	53.72	55.42	57.06	59.95
O	38.57	38.97	39.36	40.05
Totals	100.00	100.00	100.00	100.00

Table 1: Energy dispersive x-ray analysis of titanate samples.

X-ray diffraction patterns (XRD) of TNT as-synthesized samples are represented in Fig. (2). For both TN-W and TN-0.01MC, the main diffraction peaks are typical of layered titanates, especially the broad band one around 2θ = 10◦attributed to the interlayer distance. Intensity of this peak weakened in TN-0.01MC sample and getting more weakened in TN-0.1MC. It can be noted that this beak intensity is significantly weakened for the samples TN-0.01MC and TN-0.1MC as a function of increasing acid washing concentration this indicates the change in structure. This change may arise due to the ion-exchange reaction where the interlayer sodium ions are substituted by protons and, hence, a decrease in the interlayer spacing (due to smaller size of which hydrogen) may be expected that was indicated by a decrease in the peak intensity around 10◦. Similar comparative features in XRD patterns of no-acid and acid-washed TNT samples have also been found by Xiaoming Sun and Yadong Li (2003) and L. Q. Weng et al. (2006). Diffraction peaks were observed at 25.5◦, 37.8◦, 48.2◦, 54.2 and 55.4◦, assigned to metastable polymorph TiO_2 (Feist et al. 1988 ; A.nada et al. 2014)

According to the obtained XRD profiles, the chemical formula of both TN-W and TN-0.01MC samples may be $Na_xH_{2-x}Ti_3O_7\cdot{}_nH_2O$ (Edisson Morgado Jr. et al., 2006). Moreover, it has been reported that for TNT sample with low sodium content (such as 3.57 wt. %), the as-synthesized TNT was essentially a protonic layered titanate and the structure was very close to $H_2Ti_3O_7$ (Edisson Morgado Jr. et al., 2006). TN-1MC can be indexed with the coexistence of anatase and rutile phases. From both the TEM image and XRD pattern of TN-1MC, it can be concluded that when the sodium content of TNT is approximately 0 wt. % (meaning a nearly complete proton exchange), the nanotubular structure of titanates may be destroyed.

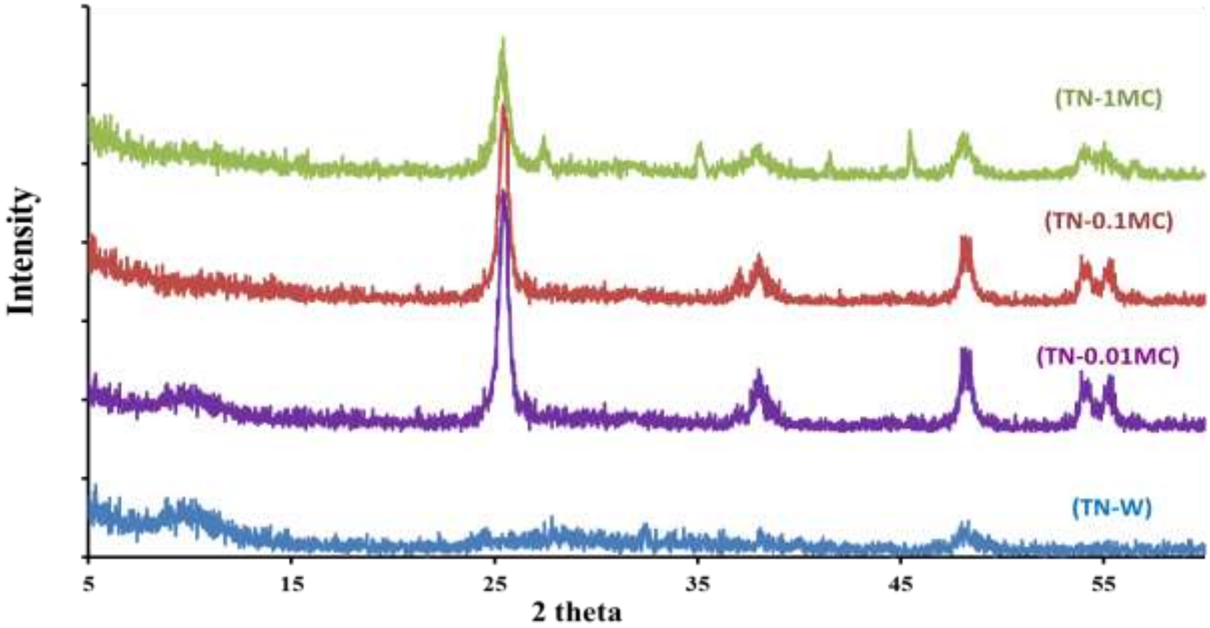

Fig. 2: XRD patterns of prepared titanate samples.

The studied samples was also followed by FT-IR analysis in the range between 4000 and 400 cm^{-1} and the results obtained have been illustrated in Fig. 3. When the IR spectra of the nanotubes samples were compared with those reported in the literature for original samples of $Na_2Ti_3O_7$ and $H_2Ti_3O_7$ (A.L. Sauvet et al., 2004; M. Latroche, 1990), the differences in peak intensities and broadening of the peaks between the original samples and nanotubes may be due to the dimensional confinement possessed by nanotubes.

A broad and intense band located around 3300–3500 cm^{-1} can be ascribed to OH stretching vibrations. The presence of this peak advocates the existence of hydroxyl groups and huge amount of water molecules in the surface and interlayer space. Vibration around 1630–1640 cm^{-1}also confirmed the presence of water and can be assigned to H–O–H bending vibrations of water (Maira et. al. 2001). The positions of the bands of the samples were more or less similar but for sample TN-W, the band around 900 cm^{-1} was prominent. The band around 900 cm^{-1} represents the stretching vibration of short Ti–O bonds involving nonbridging oxygen coordinated with sodium ions. As mentioned above, the peak for this band (900 cm^{-1}) can be seen for sample TN-W and decrease in TN-0.01MC and approaching of disappear in TN-0.1MC finally it could not be seen for sample TN-1MC (hydrogen form). The broad band (from about 800 till 400 cm^{-1}) was assigned to Ti–O and Ti–O–Ti skeletal frequency region. The sodium ions present in the samples are not only physically adsorbed but also belong to the lattice, and the composition is other than titanium dioxide (M. Qamar et. al. 2008).

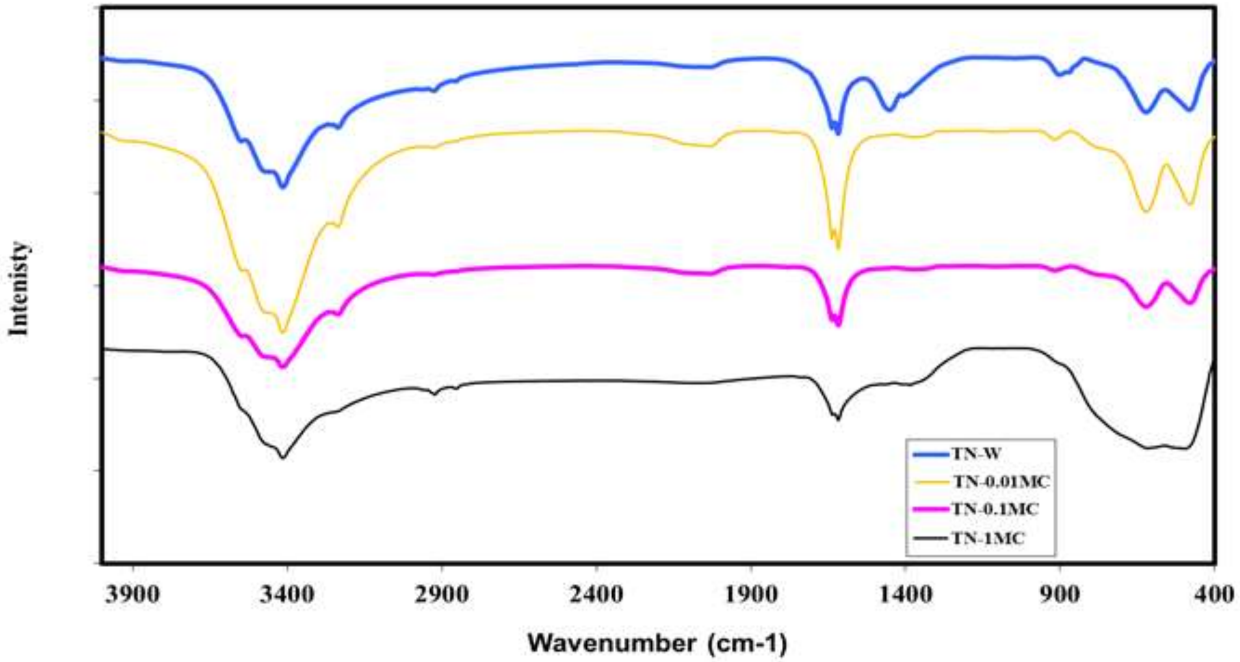

Fig. 3: FT-IR spectra of TNTs obtained and effect of Washing.

The phase transformation resulting from different post-treatments by washing was also confirmed by Raman analysis. The Raman spectra of different samples are presented in Fig. 4. For TN-W, the bands characteristic of titanium and oxygen stretching vibration were observed at 148, 196, 280, 401, 442, 515 and 644 cm^{-1}, which are in good agreement with the Raman spectrum obtained by Rongxin Mu et al. (2010). Washing with HCl led to the disappearance of Raman peaks characteristic of titanate at 280 and 455 cm^{-1} in concomitance of increasing the presence of Raman peaks at 144, 196, 399, 516 and 640 cm^{-1}, assigned to the active modes of typical anatase TiO_2 (T. Ohsaka, 1978; D. Bersani, 1998) this happen gradually with increasing of concentration of HCl and when arrive to high concentration of HCl (TN-1MC) the titanate phase disappeared and two phases appear anatase and rutile. The best sample which has two phases titanate and anatase is TN-0.01MC.

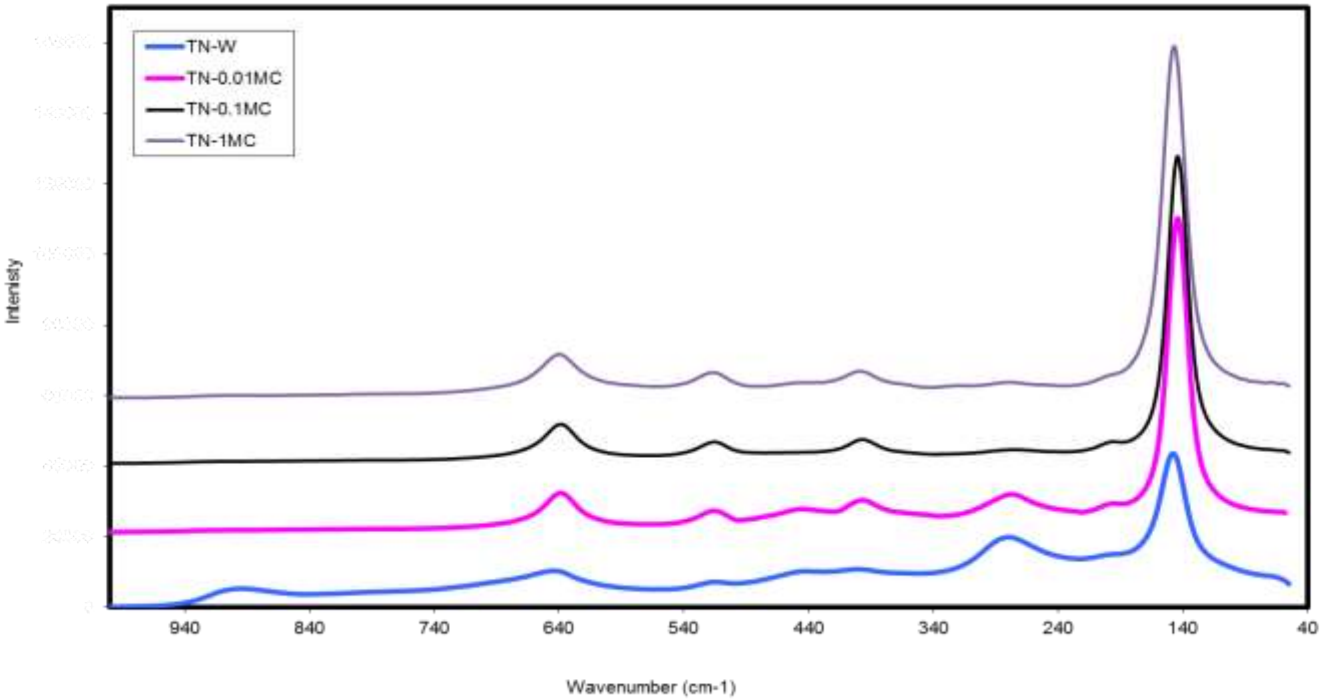

Fig. 4: Raman spectra of prepared TNTs.

The UV–visible DRS spectra were measured to investigate the optical absorption property of the samples, as shown in Fig. 5. The TNTs spectra, regardless of the samples preparation conditions, exhibit a similar course and TN-0.01MC and TN-01MC are red shifted for about 20 nm relative to TN-W. This indicates the decrease of the band gap energy. To determine the band gap energy (E_g) of the samples, the Kubelka–Munk method was used. The E_g values were calculated from the $(F(R)\, hv)^{1/2}$ versus hv plots, where $F(R) = (1-R)/2R$ (Todorova et al., 2008). The absorption edges were found to be 347 nm and 353nm, which value corresponds to the band gap energy of E_g=3.24 eV and 3.235 eV for TN-0.01MC and TN-0.1MC respectively, the band gap energy of this two samples are as the same. The absorption edge and E_g determined for TN-W were 328 nm and 3.38 eV, respectively. The absorption edge and E_g determined for TN-1MC were 360 nm and 2.9 eV, respectively. For example, Yu and Yu (J. Yu et al., 2006) reported that E_g of TNTs prepared from rutile ranged from 3.03 to 3.15 eV, depending on the hydrothermal treatment time. Such low values of E_g were associated with a high rutile content in the prepared samples so TN-1MC has low band gap due to appearance of rutile phase and this confirmed by XRD also.

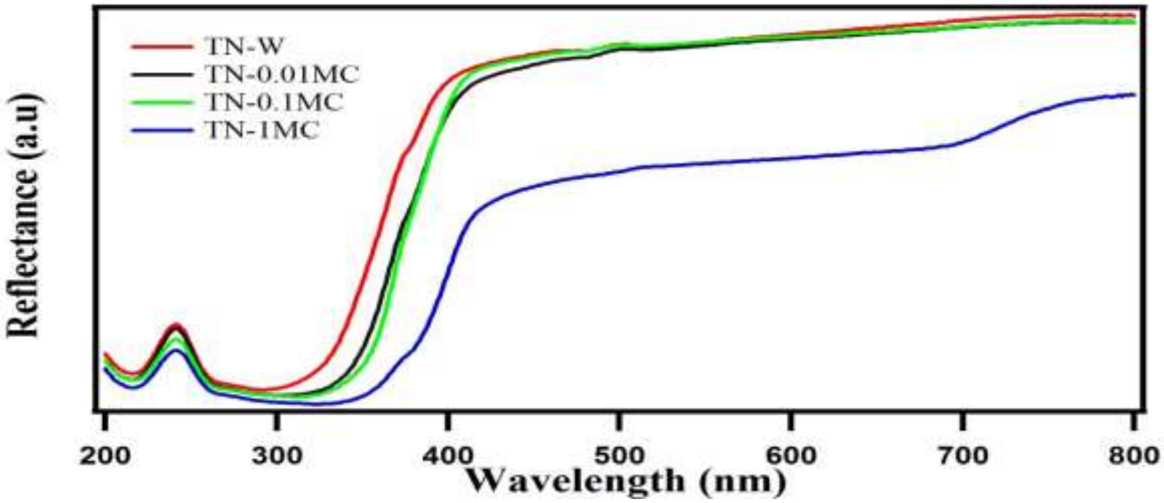

Fig. 5: UV‑vis diffuse reflectance spectra of samples

Fig. 6 shows the PL spectra of the titanate samples. The curve suggests that the electrons in the valence band are transferred to the conduction band, after which the excited electrons are stabilized by photoemission. In general, the PL intensity increases with increasing number of emitted electrons resulting from recombination between excited electrons and holes, and a consequent decrease in photoactivity (Chae, 2009; Kwak, 2009). Therefore, there is a strong relationship between the PL intensity and photoactivity In particular, the band broadening is attributed to the overlapped emission from the higher and lower excited states to the ground states. The PL intensity decreases significantly in TN-0.01MC, due to the effect of its clean surface in facilitating electron transfer and hence depressing the recombination process. Consequently, easier electron transfer activities are expected on the surface of TN-0.01MC.

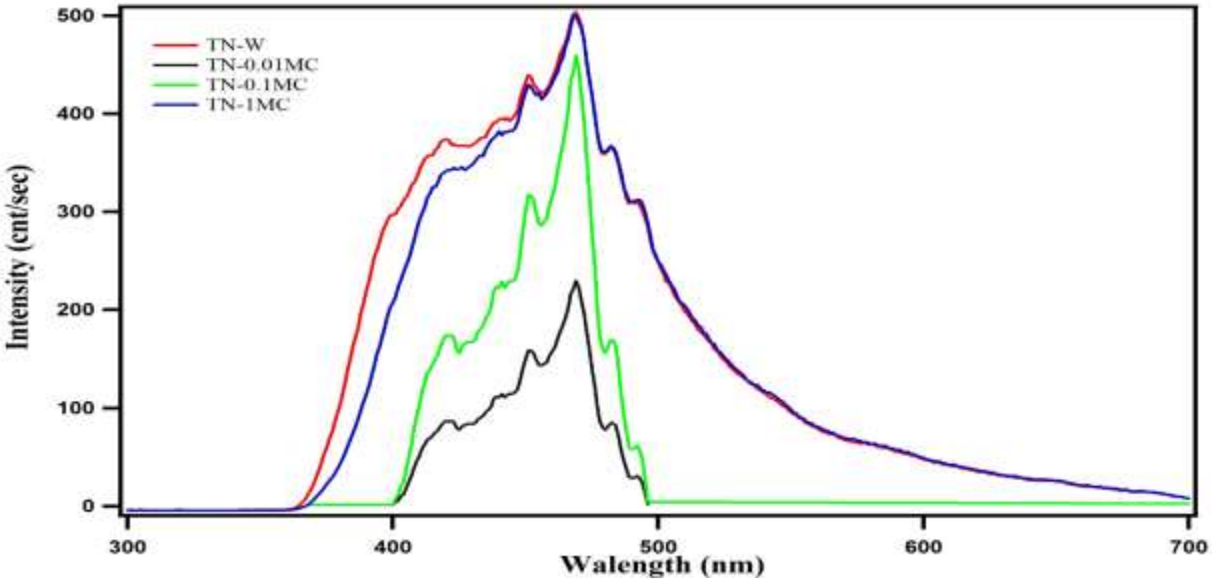

Fig. 6: Photoluminescence (PL) spectra of samples

Photocatalytic Activity

The photocatalytic degradation of aqueous phenol over the catalysts is compiled in Fig. 7. For phenol degradation overall photocatalysts, aqueous phenol concentration continuously diminished with UV irradiation, indicating that the synthesized TiO_2 nanotubes under washing with 0.01M of HCl are effective photocatalysts. However, phenol degradation efficiency varied with the structural properties of the catalysts. After UV irradiation for 300 min, phenol removal were found to be 32.8%, 72.9%, 65% and 42% for TN-W, TN-0.01MC, TN-0.1MC and TN-1MC reflecting the highest photocatalytic activity of TN-0.01MC catalysts examined.

In principle, the photocatalytic activity is closely linked to the structural properties of the photocatalyst, such as crystallinity and crystalline phase composition. The higher phenol degradation rate of TN-0.01MC compared to TN-1MC is attributed to the higher photocatalytic activity of its titanate structure (Costa and Prado, 2009).

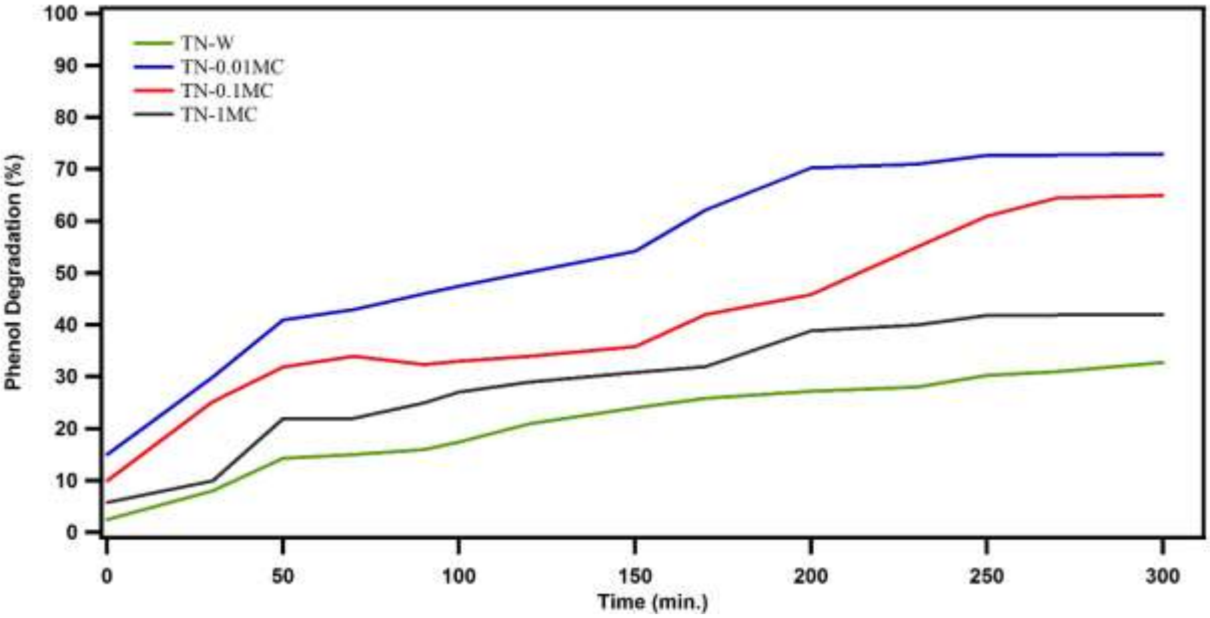

Fig. 7: The photocatalytic degradation of aqueous phenol over the catalysts.

CONCLUSIONS

Nanotubes were successfully obtained directly from a TiO_2 sol following a hydrothermal process in the presence of sodium hydroxide with and without acid washing. Sample washed with low concentration of HCl (TN-0.01MC) is the most efficient photocatalyst in this study and this sample give best result of phenol degradation. The superior activity can be attributed to it has two phases titanate and anatase, this give highly activate. Where presence of titanate with anatase give synergism effect. But in case no sodium content, TN-1MC, the photocatalytic activity decrease due to change titanate phase and the nanotubular structure becomes diffused. Without washing by HCl, TN-W, the nanotubular structure uncompleted formation.

REFERENCES

A.L. Sauvet, S. Baliteau, C. Lopez, P. Fabry; "Synthesis and characterization of sodium titanates $Na_2Ti_3O_7$ and $Na_2Ti_6O_{13}$", J. Solid State Chem., 177, 4508 (2004).

A.nada, Yasser Moustafa, Amal Hamdy, Saad Abd El-Wahab and Dena Yahea; "Synthesis and Photocatalytic Activity of Single Crystal Titanate"; Chemistry and Materials Research; 6, 40-49 (2014).

B. S. Kwak, J. Chae, J. Kim, and M. Kang, "Enhanced hydrogen production from methanol/water photo-splitting in TiO_2 including Pd component"; Bulletin of the Korean Chemical Society, 30, 1047 (2009).

Costa L.L., Prado A.G.S."; TiO_2 nanotubes as recyclable catalyst for efficient photocatalytic degradation of indigo carmine dye"; J. Photochem. Photobiol. A: Chem. 201, 45–49 (2009).

D. Bersani, P.P. Lottici, "Phonon confinement effects in the Raman scattering by TiO2 nanocrystals"; Appl. Phys. Lett. 72, 73–75 (1998).

Edisson Morgado Jr., Marco A.S. de Abreu, Oscar R.C. Pravia, Bojan A. Marinkovic, Paula M. Jardim, Fernando C. Rizzo and Antonio S. Araújo; "A study on the structure and thermal stability of titanate nanotubes as a function of sodium content"; Solid State Sciences, 8, 888-900 (2006) .

Feist T.P., Mocarski S.J., Davies P.K., Jacobson A.J., Lewandowski J.T., "Formation of TiO_2 by proton exchange and thermolysis of several alkali metal titanate structure"; Solid State Ionics, 28, 1338–1343 (1988).

Fox, M. A. and M. T. Dulay, ''Heterogeneous Photocatalysis''; Chem. Rev., 93, 341 (1993).

H. Yu, J. Yu, B. Cheng, and M. Zhou, ''Effects of Hydrothermal Post-Treatment on Microstructures and Morphology of Titanate Nanoribbons''; J. Solid State Chem., 179, 349 (2006c).

J. Chae, J. Lee, J. Jeong, M. Kang; Hydrogen Production from Photo Splitting of Water Using the Ga-incorporated TiO_2s Prepared by a Solvothermal Method and Their Characteristics; Bulletin of the Korean Chemical Society; 30,302 (2009).

J. Yu, H. Yu; "Facile synthesis and characterization of novel nanocomposites of titanate nanotubes and rutile nanocrystals"; Mater. Chem. Phys., 100,507 (2006).

J. Yu, H. Yu, B. Cheng, X. Zhao and Q. Zhang, ''Preparation and Photocatalytic Activity of Mesoporous Anatase TiO2 Nanofibers by a Hydrothermal Method''; J. Photochem. Photobiol. A, 182, 121 (2006b).

Kasuga, T., ''Formation of Titanium Oxide Nanotubes Using Chemical Treatments and Their Characteristic Properties''; Thin Solid Films, 496, 141 (2006).

Kasuga, T., M. Hiramatsu, A. Hoson, T. Sekino, and K. Niihara, ''Formation of Titanium Oxide Nanotube''; Langmuir, 14, 3160 (1998).

Kasuga, T., M. Hiramatsu, A. Hoson, T. Sekino, and K. Niihara, ''Titania Nanotubes Prepared by Chemical Processing''; Adv. Mater., 11, 1307 (1999).

L. Q. Weng, S. H. Song, S. Hodgson, A. Baker, and J. Yu, ''Synthesis and Characterisation of Nanotubular Titanates and Titania''; J. Eur. Ceram. Soc., 26, 1405 (2006).

Lee, C. K., C. C. Wang, M. D. Lyu, L. C. Juang, S. S. Liu, and S. H. Hung, ''Effects of Sodium Content and Calcination Temperature on the Morphology, Structure, and Photocatalytic Activity of Nanotubular Titanates''; J. Colloid Interf. Sci., 316, 347 (2007b).

Li Shi Wang, Ming Wei Xiao, Xin Jian Huang, Yan Dan Wu, “Synthesis, characterization, and photocatalytic activities of titanate nanotubes surface-decorated by zinc oxide nanoparticles”; Journal of Hazardous Materials, 161, 49–54 (2009).

Lin, J. and J. C. Yu, ‘‘An Investigation on Photocatalytic Activities of Mixed TiO2-rare Earth Oxides for the Oxidation of Acetone in Air’’; J. Photochem. Photobiol. A, 116, 63 (1998).

M. Latroche, L. Brohan, R. Marchand, M. Tournoux; “Cs_xTiO_2 bronzes with hollandite structure: Cationic ordering and physical properties”; 25,139 (1990).

M. Qamar, C.R. Yoon, H.J. Oh, N.H. Lee, K. Park, D.H. Kim, K.S. Lee, W.J. Lee, S.J. Kim; “Preparation and photocatalytic activity of nanotubes obtained from titanium dioxide”; Catalysis Today 131, 3–14 (2008).

Maira A.J., Coronado J.M., Augugliaro V., Yeung K.L., Conesa J.C., J.Soria, “Fourier transform infrared study of the performance of nanostructured TiO_2 particles for the photocatalytic oxidation of gaseous toluene”; J.Catal. 202, 413–420 (2001).

N. Todorova, T. Giannakopoulou, G. Romanos, T. Vaimakis, Jiaguo Yu and C. Trapalis; Preparation of fluorine-doped TiO_2 photocatalysts with controlled crystalline structure; Int. J. Photoenergy, 9, 1155 (2008).

Rongxin Mu, Zhaoyi Xu, Liyuan Li, Yun Shao, Haiqing Wan, Shourong Zheng; “On the photocatalytic properties of elongated TiO2 nanoparticles for phenol degradation and Cr(VI) reduction”; Journal of Hazardous Materials 176, 495–502 (2010).

S.S. Kanmani, K. Ramachandran, “Synthesis and characterization of TiO2/ZnO core/shell nanomaterials for solar cell applications”; Renewable Energy, 43, 149-156 (2012).

Sun, Z., Y. Chena, Q. Kea, Y. Yang, and J. Yuan, ‘‘Photocatalytic Degradation of a Cationic Azo Dye by TiO2/Bentonite Nanocomposite’’; J. Photochem. Photobiol. A: Chem., 149, 169 (2002).

T. Ohsaka, F. Izumi, Y. Fujiki, “Raman spectrum of anatase TiO_2”; J. Raman Spectrosc. 7, 321–324 (1978).

Tseng, I. H., W. C. Chang, and J. C. S. Wu, ‘‘Photoreduction of CO2 Using Sol–Gel Derived Titania and Titania-supported Copper Catalysts’’; Appl. Catal. B: Environ., 37, 37 (2002).

Xiaoming Sun and Yadong Li, “Synthesis and Characterization of Ion-Exchangeable Titanate Nanotubes”; Chemistry - A European Journal, 9, 2229-2238 (2003).

Yamashita, H., M. Harada, J. Misaka, M. Takeuchi, K. Ikeue, and M. Anpo, ‘‘Degradation of Propanol Diluted in Water under Visible Light Irradiation Using Metal Ionimplanted Titanium Dioxide Photocatalysts’’; J. Photochem. Photobiol. A: Chem., 148, 257 (2002).

Yoshida, R., Y. Suzuki, and S. Yoshikawa, ‘‘Effects of Synthetic Conditions and Heat-Treatment on the Structure of Partially Ion-exchanged Titanate Nanotubes’’; Mater. Chem. Phys., 91, 409 (2005).

Yu, J., H. Yu, B. Cheng and C. Trapalis, ‘‘Effects of Calcination Temperature on the Microstructures and Photocatalytic Activity of Titanate Nanotubes’’; J. Mol. Catal. A: Chem., 249, 135 (2006a).

Zhang, M., Z. Jin, J. Zhang, X. Guo, J. Yang, W. Li, X. Wang, and Z. Zhang, ‘‘Effect of Annealing Temperature on Morphology, Structure and Photocatalytic Behavior of Nanotubed $H_2Ti_2O_4(OH)_2$’’; J. Mol. Catal. A, 217, 203 (2004).